Colloid Polym Sci 279:459–467 (2001)

ORIGINAL CONTRIBUTION

A. Farkas
I. Dékány

Interlamellar adsorption of organic pollutants in hydrophobic montmorillonite

Received: 17 July 2000
Accepted: 5 October 2000

A. Farkas · I. Dékány (✉)
Department of Colloid Chemistry
University of Szeged
H-6720 Szeged, Aradi V.t.1. Hungary
e-mail: i.dekany@chem.u-szeged.hu

I. Dékány
Nanostructured Materials Research Group
Hungarian Academy of Science
H-6720 Szeged, Aradi V.t.1. Hungary

Abstract The adsorption of nitrobenzene, 2-chlorophenol, and 4-chlorophenol from water on organophilized derivatives of *n*-hexadecylpyridinium-montmorillonite (HDP-montmorillonite) was studied. Adsorption excess isotherms were obtained by the immersion method and were analyzed to determine the adsorption capacity of organic pollutants on the hydrophobized surface. The basal spacings of the clay minerals were determined by X-ray diffraction. The results of X-ray diffraction measurements are in good agreement with excess isotherms: whenever a region of the isotherm indicates an increase for the adsorption of organic component, an increase in basal spacing (interlamellar swelling) is also observed. By combining these two independent methods, composition and structure of the interlamellar space between the silicate layers could be accurately calculated. The free enthalpy of adsorption, the adsorption capacity, and the separation factor for adsorption are calculated by analyzing the adsorption isotherm on the basis of the Gibbs equation and Everett-Schay method. The results are utilizable for planning environmental procedures and systems (water clarification and soil remediation).

Key words Clays · Montmorillonite · Adsorption · Pollutants · Hydrophobic surface

Introduction

The adsorption of organic compounds on soil components – particularly on clay minerals – and their organophilized derivatives has lately attracted much interest [1, 2, 9, 10]. Clay minerals are among the most reactive soil components which, due to their large specific surface area and ion exchange capacity, are capable of adsorbing organic pollutants.

Our former results have greatly contributed to the progress of studies on selective adsorption from binary mixtures and solutions on clay minerals [3–12]. In the last few years studies have become increasingly focused on solutions of water with organic molecules very poorly miscible with water [9–12], not least because of their outstanding environmental significance. These solutions are excellent models for water polluted with toxic aromatic compounds. The exact description of their adsorption on clay minerals is essential for environmental protection, and the experimental results will open the way for the development of new procedures for the immobilization of pollutants in flowing systems.

The surface polarity of clay minerals is altered by hydrophobization via treatment with cationic surfactants. As a consequence, the modified minerals become capable of adsorbing organic components very effectively [13–18]. The concentration of organic molecules in the interlamellar space enclosed by the silicate lamellae can be calculated from the adsorption excess isotherm. The knowledge of experimentally determined excess isotherms also allows the calculation of thermodynamic properties of the adsorption layer at the solid/liquid interface. Using the Gibbs equation [26–29], the free enthalpy of adsorption is determined and combined with

the adsorption excesses to calculate adsorption capacities [11] which, in the case of adsorption in dilute solutions, are often impossible to determine from the Langmuir adsorption isotherm equation. Changes in interlamellar distances due to the interlamellar adsorption are monitored by X-ray diffraction (XRD) If the basal spacing is determined by XRD, one can calculate the interlamellar space volume – knowing the amount and volume of alkyl chains and using the excess isotherms – and also its composition in the entire concentration range. The combination of results obtained by two independent methods yields detailed additional information on adsorption equilibrium and on the structure of the adsorption layer.

Adsorption from solution and the structure of the interlamellar space

Adsorption on a solid/liquid interface is a displacement process. Consequently the positive adsorption of one component (i.e., the increase in its concentration in the interfacial layer) is accompanied by the negative adsorption of the other. Based on the relationships postulated by Gibbs' model of S/L interfaces, the reduced excess amount normalized to unit mass of adsorbent ($n_1^{\sigma(n)}$) and the Ostwald-de Izaguirre equation derived from the material balance of the components can be formulated in the following way [19–21]:

$$n_1^{\sigma(n)} = n^0(x_1^0 - x_1)/m = n^0\Delta x_1/m \tag{1}$$

$$n_1^{\sigma(n)} = n_1^s x_2 + n_2^s x_1 = n_1^s - n^s x_1 = n^s(x_1^s - x_1) \tag{2}$$

where n^0 is the total material amount of the liquid, x_1^0 and x_1 are the initial and equilibrium molar fraction, respectively, of component 1 in the liquid phase, m is the mass of the adsorbent, $n^s = n_1^s + n_2^s$ is the material content of the adsorption layer and $x_1^s = (1 - x_2^s) = n_1^s/n^s$ is the equilibrium molar fraction of component 1 in the adsorption layer. If component 1 is preferentially adsorbed as compared to component 2, the excess $n_1^{\sigma(n)}$ approximately equals the material amount n_1^s [19, 20]. In dilute solutions, in the case of preferential adsorption of the dissolved material, the volume of the dissolved material in the adsorption layer is approximately $V_1^s = n_1^s V_{m,1} \approx n_1^{\sigma(n)} V_{m.1}$ [3–5]. The adsorption capacity of pure component 1 is

$$n_{1,0}^s = n_1^s + rn_2^s = n^s x_1^s + rn^s x_2^s \tag{3a}$$

where $r = V_{m,2}/V_{m,1} = n_{1,0}^s/n_{2,0}^s$, i.e., the ratio of the molar volumes of the pure components. After the introduction of the separation factor $S = x_1^s x_2/x_2^s x_1$ the equation

$$n^s = n_{1,0}^s[Sx_1 + x_2]/[Sx_1 + rx_2] \tag{3b}$$

is obtained for the material content of the adsorption layer. The value of $n_{1,0}^s$ may be determined from the slope and the intersection of the Everett-Schay linear representation [22–25], i.e.,

$$\frac{x_1 x_2}{n_1^{\sigma(n)}} = \frac{1}{n_{1,0}^s}\left[\frac{r}{S-1} + \frac{S-r}{S-1}x_1\right] \tag{4}$$

Using the integrated form of the Gibbs equation describing solid/liquid interfaces [26–29], the free enthalpy of adsorption can be formulated in the following way:

$$\Delta_{21}G = -RT\int_0^{x_1} \frac{n_1^{\sigma(n)}}{(1-x_1)x_1}\left(1 + \frac{\mathrm{d}\ln\gamma_1}{\mathrm{d}\ln x_1}\right)\mathrm{d}x_1 \tag{5}$$

The index "$_{21}$" indicates that the molecules of component 2 are exchanged for those of component 1 and γ_1 is the activity coefficient of component 1 in the bulk phase. In ideal solutions or in solutions considered to be ideally dilute (like our systems), the value of the parenthetic term containing the derivative of the activity coefficient is 1. Using the molar free enthalpies of the components (g_i^s), the equation $\Delta_{21}G = n_1^s\left(g_1^s - g_2^s/r\right)$ holds for the entire concentration range. After combination with Eqs. (2) and (5) and appropriate rearrangements, the following relationship is obtained [5]:

$$\frac{\Delta_{21}G}{n_1^{\sigma(n)}} = \Delta_{21}g + n^s\Delta_{21}g\frac{x_1}{n_1^{\sigma(n)}} \tag{6}$$

The linear representation of the equation yields the molar free enthalpy of adsorption, $\triangle_{21}g$ and the material content of the interfacial layer, n^s. The volume per unit cell of the alkyl chains hydrophobizing the silicate layer (in units of $\mathrm{nm}^3/[\mathrm{Si,Al}]_4\mathrm{O}_{10}$) for *n*-alkylpyridinium montmorillonite as the adsorbent is

$$V_{\mathrm{alk}} = \{0.205[0.127(n_{\mathrm{C-C}} + n_{\mathrm{C-N}}) + 0.28] + 0.118\}\zeta \tag{7}$$

The parenthetic term expresses the length in nm of the alkyl chains attached to the surface. ($n_{\mathrm{C-C}}$ and $n_{\mathrm{C-N}}$ are the number of carbon-carbon and carbon-nitrogen bonds, respectively.) The cross-section of the straight-chain aliphatic hydrocarbon chain is 0.205 nm^2. V_{alk} includes the volume of the pyridine ring (0.118 nm^3). The number of charges per formal unit (surface charge density, $\omega = 0.32$) may be obtained from the concentration of alkyl chains by thermogravimetric analysis. The thickness of the silicate layer is 0.96 nm and the surface of the base of the formal unit is 0.232 nm^2; thus the interlamellar volume may be formulated in the following way [3, 4]:

$$V_{\mathrm{int}} = 0.232(d_L - 0,96)(\mathrm{nm}^3/[\mathrm{Si,Al}]_4\mathrm{O}_{10}) \tag{8}$$

The volume of the "free" interlamellar space is the difference $V_{\mathrm{int}} - V_{\mathrm{alk}}$

$$V_{\text{int}} - V_{alk} = V_1^s + V_2^{s,b} \quad (9a)$$

$$1 = \Phi_{alk} + \Phi_1^s + \Phi_2^{s,b} \quad (9b)$$

where $V_2^{s,b} = V_2^s + V^b$ is the combined volume of the water molecules present in the adsorption layer and the so-called bulk liquid, filling the adsorption space [10]. The latter does not participate in the formation of the adsorption layer; it is, however, controlled by the forces of adsorption, like all molecules in the interlamellar space. Due to preferential adsorption of the dissolved material, V^b consists mostly of water, which is the reason why it may be combined with V_2^s. Dividing of Eq. (9a) by V_{int} and subsequent rearrangement yield Eq. (9b) for the volume fractions of the alkyl chain, Φ_{alk} and the components, Φ_i^s. Representation of Φ_i^s as a function of the equilibrium concentration, or the real volume fraction of the bulk phase, gives a demonstrative view of the interlamellar concentrations of the various components of the system.

Materials and methods

Liquid sorption experiments

The dilute solutions studied were saturated solutions of pollutant aromatic pollutant (nitrobenzene, 2-chlorophenol, and 4-chlorophenol = component 1, distilled water = component 2) and a series of dilutions made thereof (at 10–12 points in the range of $x_{1,\text{relative}} = x_{1,\text{saturation}} = 0$–1). Saturated solutions were made up at 20 ± 0.5 °C by addition of the organic compounds to distilled water under continuous mechanical shaking, for a saturation time of 2 weeks. The upper, aqueous phase of lower density is the stock solution, which was stored in a dark bottle for protection against photodecomposition.

Adsorption of the solution series obtained was studied on *n*-hexadecylpyridinium montmorillonite (HDP-montmorillonite) as the adsorbent. The original montmorillonite samples (Mád, Tokaj mountains, Hungary, cec (cation exchange capacity) = 0.851 mmol/g) were organophilized at 338 K by the addition of the cationic surfactant (hexadecylpyridinium chloride) in a 1.5-fold amount related to the cec (i.e., 150% of the cec was added from the cationic surfactant to the montmorillonite suspension). The ion exchange time was 48 h. The samples were washed with 1:1 propanol-water mixture, dried and pulverized [3, 4, 11].

The adsorption excess isotherms were determined by the immersion method. Known volumes (9 cm^3) of the solution were added to 0.03–0.3 g of the HDP-montmorillonite. After equilibration the samples were centrifuged. The concentration of the supernatant and the original solution was determined by a Zeiss liquid interferometer [3–5].

X-ray diffraction measurements

The XRD experiments were carried out in a Philips X-ray diffractometer (PW 1930 generator, PW 1820 goniometer) with CuK-α radiation ($\lambda = 1.5418$) at $2\Theta = 1$–10°. In order to prevent the evaporation of the aquatic solution, the hydrophobic clay suspension in equilibrium solution was coated by a thin Mylar foil. The basal spacing (d_L) was calculated from the (001) reflexion by the Bragg equation.

Results and discussion

In the systems studied in this work, adsorption on the HDP-montmorillonite is positive (preferential) with respect to the organic component in the entire composition range: in other words, the interfacial layer is enriched in aromatic molecules. For example, adsorption from an aqueous solutions of nitrobenzene reaches saturation at an adsorption excess around $n_1^{\sigma(n)} = 0.9$ mmol/g (Fig. 1a). The course of adsorption is significantly affected by the surface polarity of the clay mineral, since on surfaces of polar character either the entire adsorption isotherm or its initial segment indicates preferential adsorption of water. As an example the adsorption of nitrobenzene from aqueous solutions is shown for Ca-montmorillonite (Fig. 1b). The initial segment of the excess isotherm shows preferential adsorption of water (negative adsorption

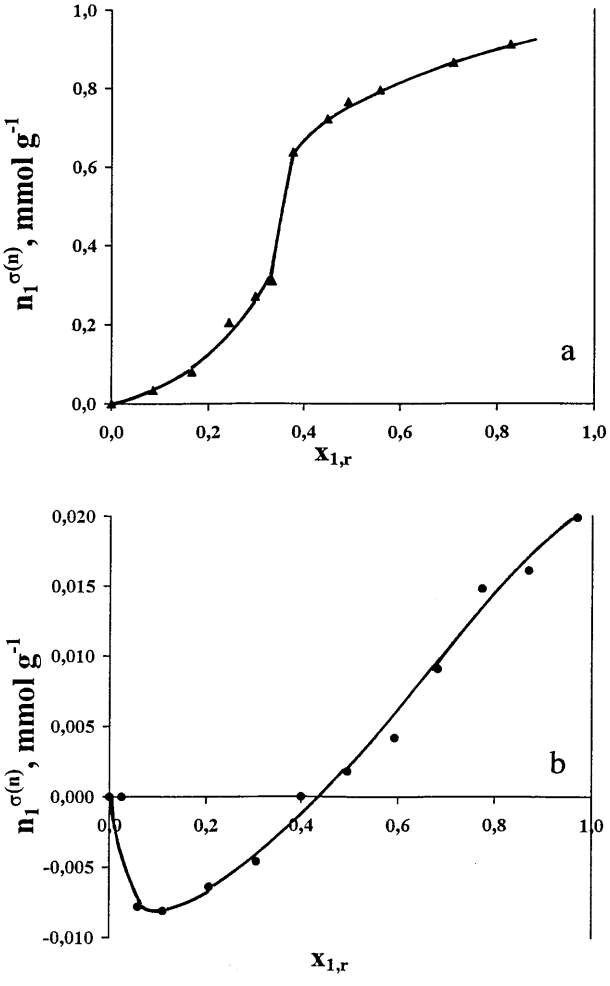

Fig. 1 **a** Adsorption excess isotherms of nitrobenzene from water on HDP-montmorillonite (▲). **b** Adsorption excess isotherms of nitrobenzene from water on Ca-bentonite (●)

for nitrobenzene). Only at nitrobenzene concentrations higher than a molar fraction of $x_{1,r} = 0.4$, i.e., at the azeotropic composition, the organic molecule is preferentially adsorbed. The reason behind this phenomenon is the excellent hydratation of Ca^{2+} ions and the hydrophilic character of the surface.

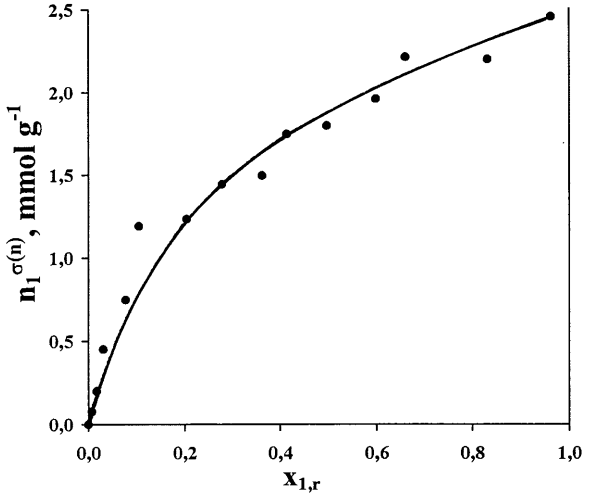

Fig. 2 Adsorption excess isotherm of 2-chlorophenol from water on HDP-montmorillonite

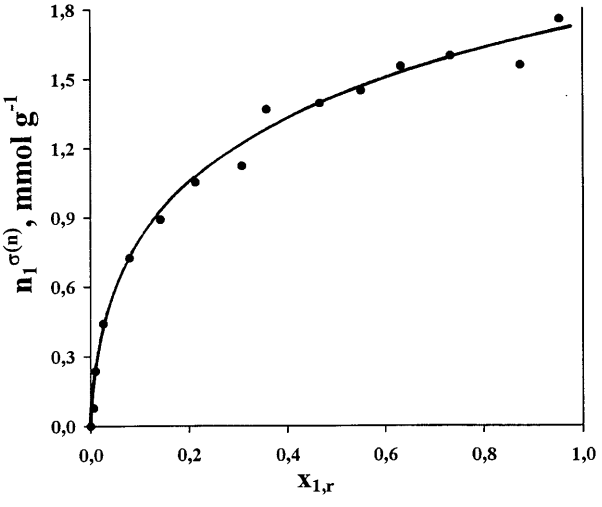

Fig. 3 Adsorption excess isotherm of 4-chlorophenol from water on HDP-montmorillonite

The value of adsorption excess in the vicinity of saturation concentration is 2.5 mmol/g and 1.8 mmol/g for adsorption of 2-chlorophenol (Fig. 2) and 4-chlorophenol (Fig. 3), respectively, from aqueous solution. The isotherms of the two chlorophenol isomers have similar shapes; the reason for the slightly higher adsorption of 2-chlorophenol is that this molecule is more polarizable and is therefore adsorbed in the interlamellar space to a higher extent.

Adsorption capacities calculated using the Everett-Schay linear representation (Eq. 4) are $n^s_{1,0} = 2.86$ mmol/g for 2-chlorophenol and 1.99 mmol/g for 4-chlorophenol (Fig. 4). The adsorption capacity calculated from the excess isotherm of nitrobenzene is $n^s_{1,0} = 1.27$ mmol/g (Table 1).

The free enthalpy functions determined according to Gibbs' equation (Eq. 5) are plotted against relative molar fractions in Fig. 5. The change in free enthalpy accompanying the adsorption of the chlorophenols is quite considerable, 9.5 J/g and 11.6 J/g, while it is as low as 2.8 J/g for nitrobenzene. When values of $\triangle_{21}G$ are plotted against the absolute molar fractions (Fig. 5b), it becomes obvious that the three functions increase in a similar way; due to the poor solubility of nitrobenzene, however, in the nitrobenzene/water system demixing occurs at a considerably lower concentration, making

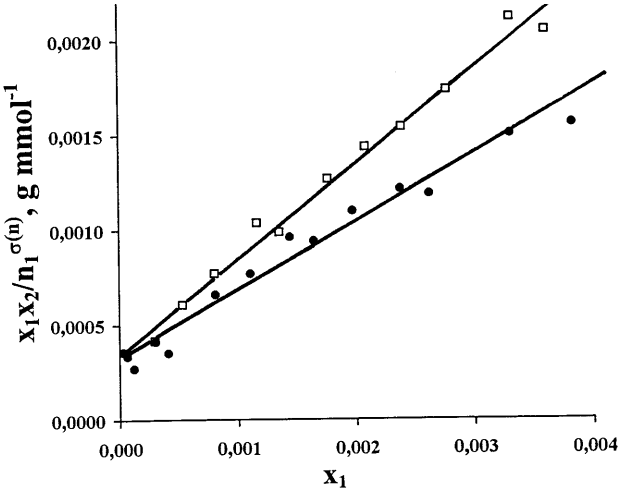

Fig. 4 Everett-Schay representation of adsorption excess isotherms (2-chlorophenol-water (●) and 4-chlorophenol-water (□) on HDP-montmorillonite)

Table 1 The adsorption capacity from the Everett-Schay representation, adsorption excess and free energy data and the separation factor S_{sep}

Pollutant	$n^s_{1,0}$, mmol g^{-1} (Eq. 4)	n^s, mmol g^{-1} (Eq. 6)	$-\triangle_{21}G$, J mmol^{-1} (Eq. 6)	S_{sep} ($x_1 = 0{,}0002$)	S_{sep} ($x_1 = 0{,}002$)
Nitrobenzene	1.27	–	–	360	–
2-Chlorophenol	2.86	0.94	3.59	230	40
4-Chlorophenol	1.99	0.97	3.85	210	30

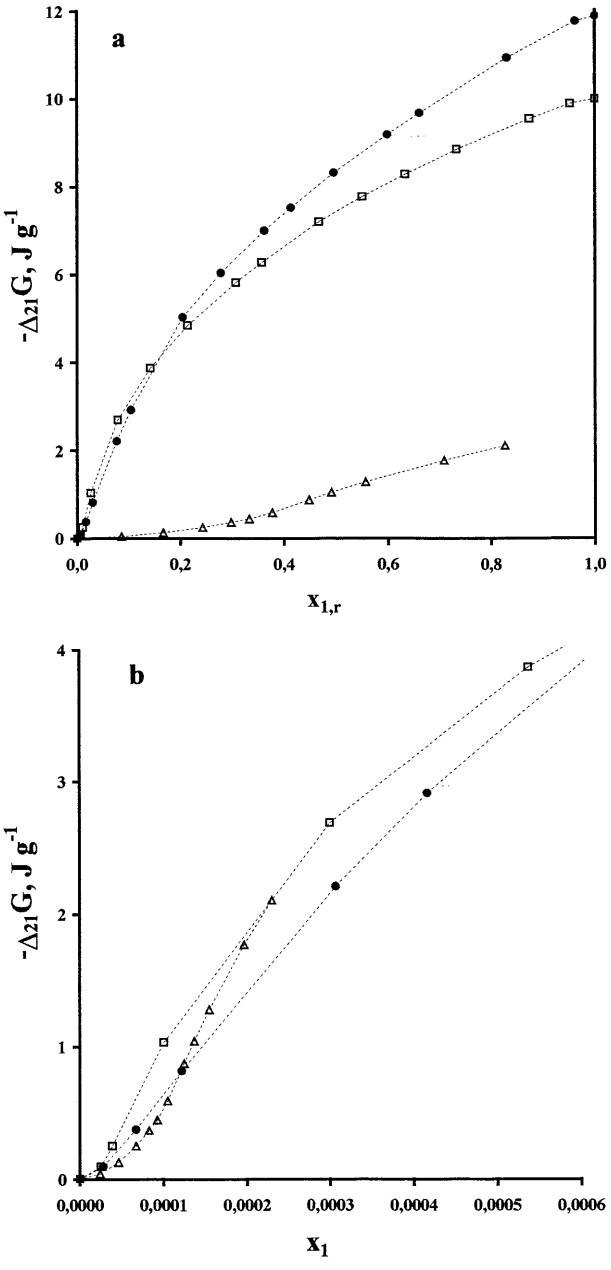

Fig. 5 **a** Free enthalpy of adsorption in 2-chlorophenol (●)-, 4-chlorophenol (□)-, and nitrobenzene (△)-water on HDP-montmorillonite (plotted against $x_{1,r}$). **b** The first section of thermodynamic function is also plotted against x_1

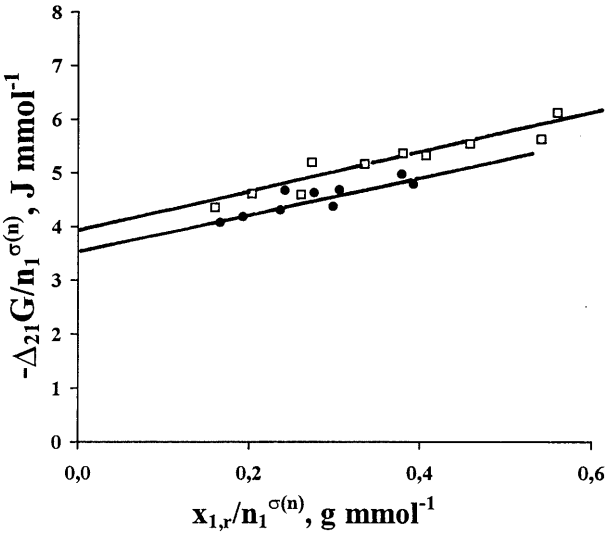

Fig. 6 Combination of adsorption excess and free enthalpy data on HDP-montmorillonite in 2-chlorophenol-water (●) and 4-chlorophenol-water (□)

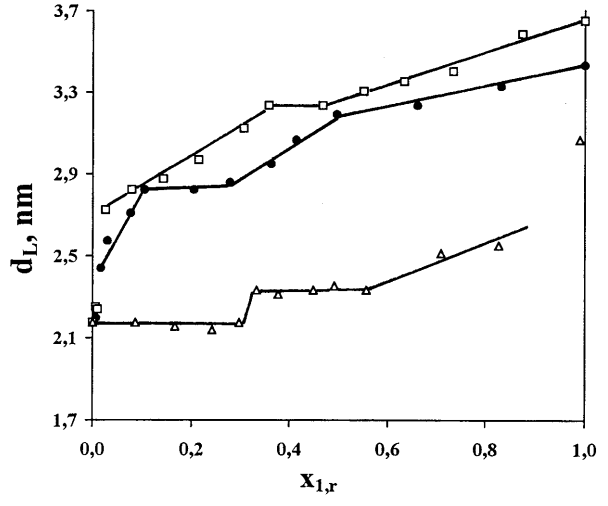

Fig. 7 Basal spacings of HDP-montmorillonite in aqueous solution of 2-chlorophenol-water (●), 4-chlorophenol-water (□), and nitrobenzene-water (△)

Table 2 Calculated and experimental basal spacings of HDP-montmorillonite in water and in different solutions

Hydrophobic HDP Montmorilonite	Aquatic solution	Calculated d_L, nm	Experimental d_L, nm
Dry		1.86 ($\alpha = 0°$)	1.77
Suspended in water		2.29 ($\alpha = 35°$, monolayer)	2.18
In saturated solution of	Nitrobenzene		3.06
	2-Chlorophenol	3.61 ($\alpha = 35°$, bilayer)	3.43
	4-Chlorophenol		3.65

the calculation of further data at higher concentrations impossible.

Based on the free enthalpy function, the representation $\Delta_{21}G/n_1^{\sigma(n)} = f(x_1/n_1^{\sigma(n)})$ can also be drawn, yielding the values of molar free enthalpies and n^s (Fig. 6, Table 1). The change in molar free enthalpy of adsorption determined from the linear representation is characteristic of the water/pollutant exchange. This enthalpy change is larger for 4-chlorophenol than for 2-chlorophenol. (In the case of nitrobenzene this function may not be used for the above evaluation, since – due to the

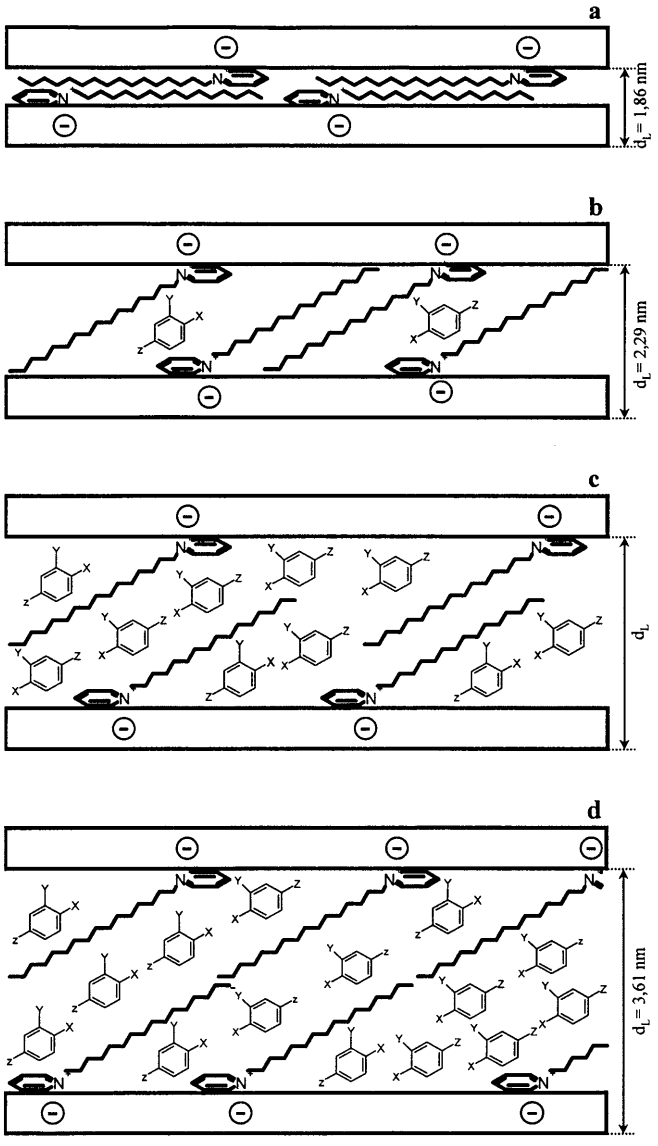

Fig. 8a–d Schematic structure of HDP-montmorillonite with increasing concentration of the pollutant (nitrobenzene: x = NO_2, y = H, z = H; 2-chlorophenol: x = OH, y = Cl, z = H; 4-chlorophenol: x = OH, y = H, z = Cl)

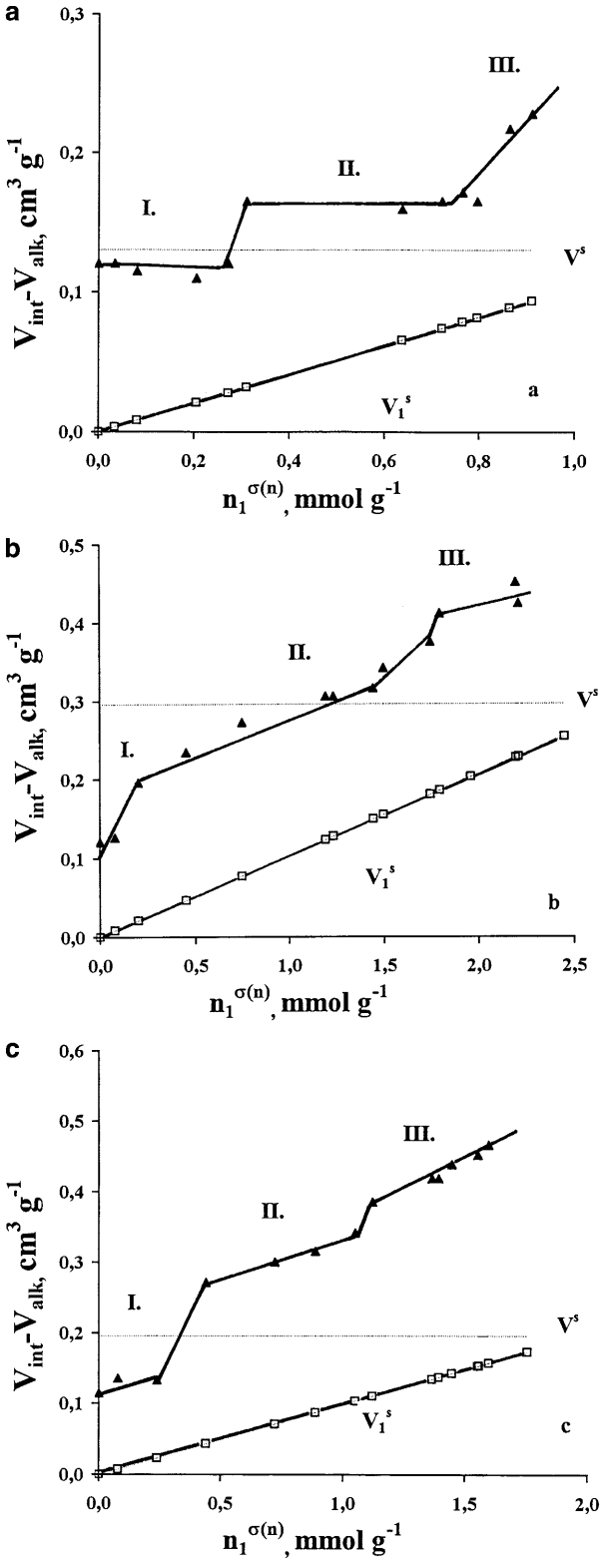

Fig. 9 **a** $V_{int} - V_{alk}$, V^s, and V_1^s for HDP-montmorillonite in nitrobenzene-water. **b** The same as a for HDP-montmorillonite in 2-chlorophenol-water. **c** The same as a for HDP-montmorillonite in 4-chlorophenol-water

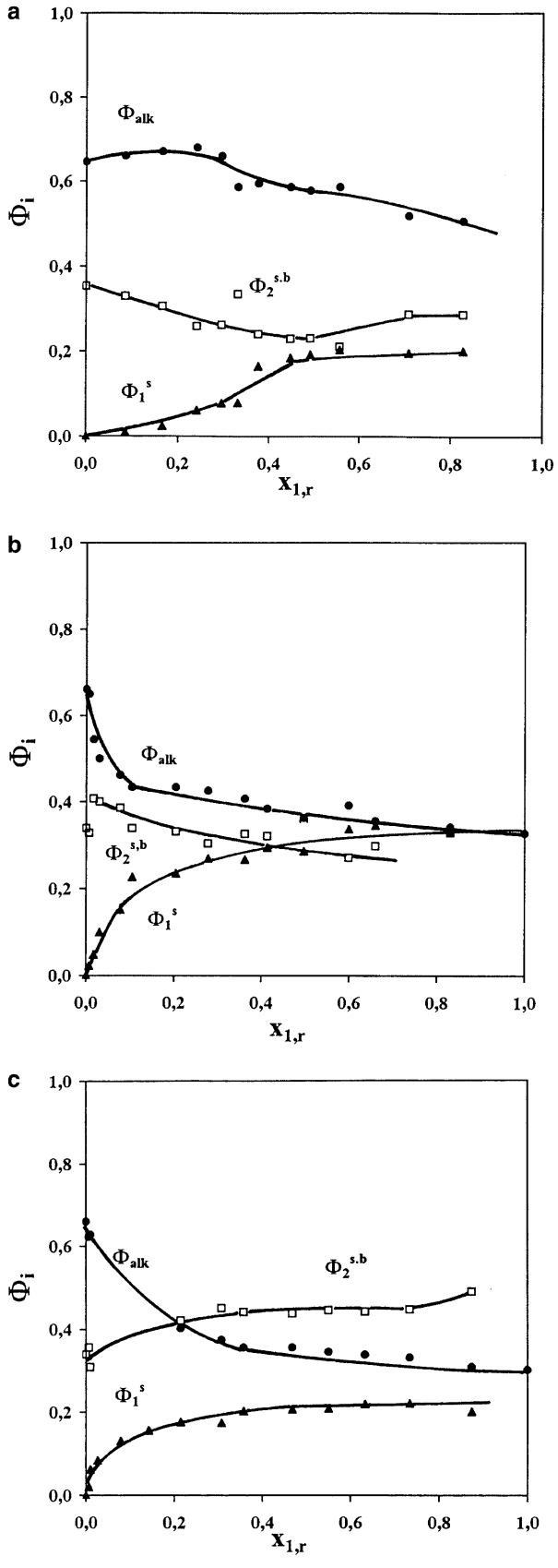

weaker adsorption interactions – the slope of the initial segment of the isotherm is too small.)

Changes of the basal spacing of HDP-montmorillonites as a function of relative molar fraction of the solution are shown in Fig. 7. The excess isotherms are in good correlation with the results of the X-ray diffraction measurements: a significant increase of basal spacing is observed in each system and the breakpoints of the curve are in accordance with the increase of the adsorption excess. The increase is caused by the intercalation of aromatic molecules in the interlamellar space. The layers, together with the alkyl chains bound to them, move apart while the concentration of the organic component in the adsorption layer increases. Due to the para position of the chlorine atom, the size of the 4-chlorophenol molecule is larger than that of 2-chlorophenol and expands the interlamellar space by 0.2–0.3 nm in comparison with the ortho compound.

As shown in Fig. 8, the expansion of the interlamellar space proceeds in three steps, corresponding to three interlamellar phases. In the dry state the alkyl chains are lying between the silicate layers (Fig. 8a). The basal spacing in Fig. 8b calculated on the basis of Eqs. (7) and (8): $d_L = [[0.127(n_{C-C} + n_{C-N}) + 0.28]\sin 35° + 0.96] = 2.29$ nm, assuming that the orientation of the alkyl chains is 35° [30]. At low relative molar fractions the aromatic molecules form a monomolecular adsorption layer in the interlamellar space. An intermediate stage is shown in Fig. 8c where the alkyl chains overlap only partially; further aromatic molecules can be intercalated and now form multimolecular layers.

In Fig. 8d, the calculated basal spacing is $d_L = [2[0.127(n_{C-C} + n_{C-N}) + 0.28]\sin 35° + 0.96] = 3.61$ nm, assuming a 35° bilayer orientation of the organophilic cations in the interlamellar space. In this case as many as four aromatic compound layers may be formed, depending on the size of the aromatic molecules.

These theoretical calculations are corroborated by our experimental results. The basal spacings measured by X-ray diffraction are: 2.18 nm in water, 3.06 nm for nitrobenzene close to saturating concentration, 3.43 nm for 2-chlorophenol, and 3.65 nm for 4-chlorophenol (Table 2). This means that the bilayer orientation is indeed established in the case of 4-chlorophenol, while in the two other systems the organophilic chains partially overlap.

The results of adsorption and X-ray diffraction measurements may be combined by plotting the change

◀

Fig. 10 Composition of the interlamellar space of the HDP-montmorillonite in nitrobenzene-water. **b** Composition of the interlamellar space of the HDP-montmorillonite in 2-chlorophenol-water. **c** Composition of the interlamellar space of the HDP-montmorillonite in 4-chlorophenol-water

in the so-called "free" interlamellar space ($V_{int} - V_{alk}$) (see Eq. 9a) against the material excess of the adsorption layer (Fig. 9) and may also be compared with the volumes $V^s = n_{1,0}V_{m,1}$ calculated from the Everett-Schay representation. This representation allows us to follow the progressing changes in the interlamellar volume, brought about by the excess being adsorbed. The first molecules are adsorbed mainly on the external surfaces and in the monomolecular layer. The interlayer space expands only slightly (stage I). When the concentration of the solution is further increased, the available volume is suddenly expanded and, as the alkyl chains no longer span the space separating the layers, aromatic molecules have easy access to the space around the hydrophobic chains and the basal spacing increases to the second plateau. Stage II is followed by continuous expansion until the system reaches the saturation concentration. This mechanism is supported by the phenomenon observed in the case of the relatively concentrated chlorophenols (Fig. 9b): within such a stage, V_2^s or V^s in the adsorption space is practically constant while the amount of organic matter steadily increases.

Calculations concerning the structure of the interlamellar space (Eqs. 7–9) and examination of the diagrams of interlamellar compositions (Fig. 10) reveal the ratio of the various components (alkyl chains, organic component, water) filling the available space. The above concept of the adsorption layer structure is also supported by the fact that the volume fraction for water $\Phi_2^{s,b}$ is larger in water/4-chlorophenol than in water/2-chlorophenol, i.e., when 4-chlorophenol is adsorbed, more water is retained in the interlamellar space. The reason for this is that the extent of interlamellar swelling is larger when 4-chlorophenol is adsorbed than in the case of 2-chlorophenol. The adsorption isotherms reveal that higher amounts of 2-chlorophenol are adsorbed than of 4-chlorophenol, in spite of the fact that the expansion of the interlayer space is smaller in the case of 2-chlorophenol. Thus, the interlamellar space "opens" wider by 4-chlorophenol, but – due to its smaller adsorption – more water is incorporated than in the case of 2-chlorophenol.

The extent of the enrichment of the organic pollutant can be characterized by the ratio $S_{sep} = [\Phi_1^s/(1-\Phi_{alk})]/\Phi_1$. This value varies as a function of concentration (Fig. 11). S_{sep} is a descriptive measure of the ratio between the volume occupied by component 1 of the liquid phase adsorbed in the interlamellar space and the volume of the bulk phase. This ratio reaches its maximum at low molar fractions of the aromatic component and can be as high as 600–800. Among the three aromatic molecules, nitrobenzene has the highest S_{sep} values (Table 1); in this system, however, phase separation occurs at low concentrations. The two chlorophenol isomers yield similar curves; S_{sep} is slightly higher for 2-chlorophenol as a consequence of the higher extent of adsorption.

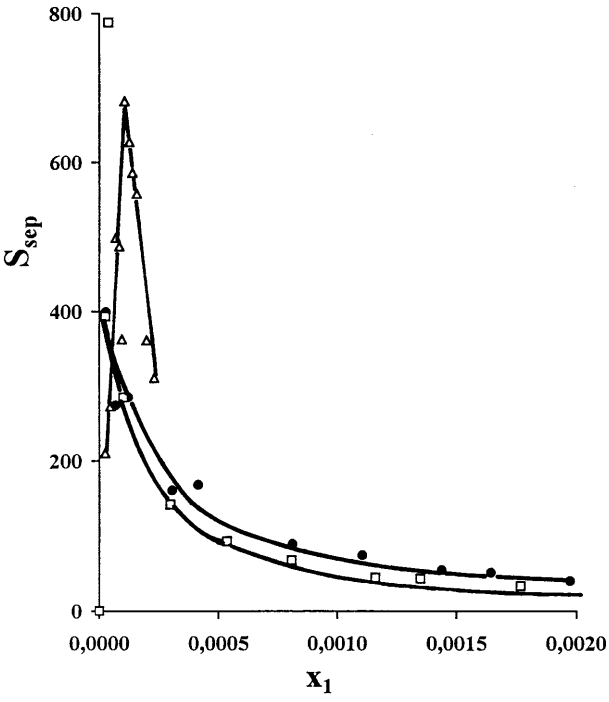

Fig. 11 Separation factor S_{sep} for 2-chlorophenol (●)-water, 4-chlorophenol (□)-water, and nitrobenzene (△)-water on HDP-montmorillonite in aqueous solutions

Conclusions

In summary, nitrobenzene and chlorophenols are adsorbed from aqueous solutions on montmorillonite hydrophobized with a cationic surfactant. Analysis of the isotherms reveals that the extent of adsorption depends on the adsorption of pollutant molecules in the interlamellar space and on how they solvate the alkyl chains of the cationic surfactant. As a consequence, an ordered interlamellar structure develops, with phase transitions in three stages: (i) a monolayer orientation at low pollutant concentrations with pollutant molecules replacing water molecules; (ii) a state intermediate between mono- and bilayer orientation where the alkyl chains overlap (Fig. 8); (iii) a bilayer orientation with the alkyl chains solvated by pollutant molecules. According to the composition diagrams, the water content is 25–35%; the rest of the interlamellar material is made up of organic molecules. The basal spacing ranges from 3.06 nm to 3.65 nm, depending on the structure of the pollutant and the adsorbed material amount.

Acknowledgements This work has been partially supported by Hungarian National Scientific Foundation (OTKA)T 025392 and Ministry of Education FKFP 0402/1999.

References

1. Klumpp E, Heitmann H, Lewandowski H, Schwuger MJ (1992) Prog Colloid Polym Sci 89:181–185
2. Schieder D, Dobias B, Klumpp E, Schwuger MJ (1994) Colloid Surf 88:103–111
3. Marosi T, Dékány I, Lagaly G (1992) Colloid Polym Sci 270:1027–1034
4. Marosi T, Dékány I, Lagaly G (1994) Colloid Polym Sci 272:1136–1142
5. Regdon I, Király Z, Dékány I, Lagaly G (1994) Colloid Polym Sci 272: 1129–1135
6. Lagaly G, Witter R (1982) Ber Bunsenges Phys Chem 86:74–83
7. Dékány I, Szántó F, Weiss A, Lagaly G (1985) Ber Bunsenges Phys Chem 89:62–67
8. Dékány I, Szántó F, Weiss A, Lagaly G (1986) Ber Bunsenges Phys Chem 90:427–431
9. Dékány I, Farkas A, Király Z, Klumpp E, Narres HD (1996) Colloid Surf A119:7–13
10. Dékány I, Farkas A, Regdon I, Klumpp E, Narres HD, Schwuger MJ (1996) Colloid Polym Sci 274:981–988
11. Regdon I, Dékány I, Lagaly G (1998) Colloid Polym Sci 276:511–517
12. Regdon I, Király Z, Dékány I, Lagaly G (1998) Prog Colloid Polym Sci 109:214–225
13. Barrer RM, Brummer K (1963) Clays Clay Miner 3:959–967
14. German WL, Harding DA (1969) Clays Clay Miner 8:213–221
15. Stul MS, Mortier WJ (1974) Clays Clay Miner 22:391–397
16. Stul MS, Maes A, Uytterhoeven JB (1978) Clays Clay Miner 26:309–320
17. Stul MS, Uytterhoeven JB, De Bock J, Huykens PL (1979) Clays Clay Miner 27:377–389
18. Stul MS, De Bock J (1985) Clays Clay Miner 33:350–357
19. Kipling JJ (1965) Adsorption from solution of non-electrolytes. Academic Press, London, p 58
20. Schay G (1969) In: Matijevic E (ed) Surface and colloid science, vol 2. Wiley, London, p 155
21. Everett DH (1972) IUPAC manual appendix II. Butterworth, London
22. Schay G (1970) In: Everett DH (ed) Proceedings of the International Symposium on Surface Area Determination. Butterworth, London, p 273
23. Fóti G, Nagy LG, Schay G (1974) Acta Chim Acad Sci Hung 80:25–32
24. Schay G, Nagy LG (1972) J Colloid Interface Sci 38:302–315
25. Everett DH (1965) Trans Faraday Soc 61:2478–2489
26. Everett DH (1997) In: Everett DH (ed) Colloid science, vol 3. Chemical Society, London, p 66
27. Schay G (1976) Pure Appl Chem 48:373–388
28. Everett DH (1981) Pure Appl Chem 53:2181–2196
29. Király Z, Dékány I (1988) Colloid Surf 34:1–12
30. Lagaly G, Stange H, Weiss A (1972) Kolloid Z Z Polym 250:675–687